# The crystal structures of delta and delta* nitrogen

# The crystal structures of $\delta$ and $\delta^*$ nitrogen

G. W. Stinton,[a] I. Loa, L. F. Lundegaard, and M. I. McMahon
*SUPA, School of Physics and Astronomy and Centre for Science at Extreme Conditions, The University of Edinburgh, Mayfield Road, Edinburgh EH9 3JZ, United Kingdom*

(Received 28 June 2009; accepted 21 July 2009; published online 14 September 2009)

The crystal structures of the high-pressure $\delta$ and $\delta^*$ phases of nitrogen have been investigated using single-crystal x-ray diffraction. The structure of the $\delta$ phase is very similar to isostructural $\gamma$-$O_2$ and comprises spherically disordered molecules, with a preference for avoiding pointing along the cubic $\langle 100 \rangle$ directions, and disklike molecules with a uniform distribution of orientations. The structure of the $\delta^*$ phase is tetragonal and the space group is identified unambiguously as $P4_2/ncm$ with unit cell parameters of $a=8.603(5)$ Å and $c=5.685(5)$ Å at 14.5 GPa. The orientations of the partially disordered molecules have been experimentally determined for the first time and are similar to those predicted on the basis of molecular dynamics simulations. © *2009 American Institute of Physics*. [doi:10.1063/1.3204074]

## I. INTRODUCTION

Nitrogen is one of seven elements that form dimers under ambient conditions, and these simple systems allow the changing nature of bonding with temperature and pressure to be probed more directly than more complex molecules. Nitrogen is of particular interest since it possesses the strongest intramolecular forces of this set with a dissociation energy of 9.8 eV.[1] Despite these strong bonds, both an amorphous phase[2] ($\eta$, see Fig. 1) and an ordered, extended solid phase[3] (Cg in Fig. 1) have been found experimentally above 1 Mbar.

At lower pressures, ten molecular phases have been reported, as shown in Fig. 1. On compression at room temperature, nitrogen crystallizes at 2.4 GPa (Ref. 4) into the hexagonal $\beta$-phase. This phase is also observed at ambient pressure at temperatures below 63 K. The structure of $\beta$-$N_2$ has space group $P6_3/mmc$ and two molecules per unit cell and comprises hexagonally close-packed three-dimensionally (3D) disordered molecules with a $c/a$ ratio very close to the "ideal" value of 1.633. This suggests true spherical disorder, although Press and Hüller[5] noted that distinguishing between a molecule precessing around the $c$-axis at the "magic angle" of 54.7° and complete spherical disorder would be very difficult, even with ideal neutron diffraction data.

On further compression to 4.9 GPa,[4] the $\beta$-phase transforms to the cubic $\delta$-phase which has space group $Pm\bar{3}n$ and eight molecules per unit cell.[6–8] The basic structure was determined by Cromer *et al.*[6] and is shown in Fig. 2(a). The nitrogen molecules exhibit two types of orientational disorder. The first set of molecules are centered on the 2*a* Wyckoff sites at (0,0,0) and $(\frac{1}{2},\frac{1}{2},\frac{1}{2})$ and have sphere-like disorder. The second type of molecules are centered on the 6*d* Wyckoff sites at $(0,\frac{1}{4},\frac{1}{2})$ and its symmetry equivalents and have disklike disorder. These two different sets of molecules will henceforth be referred to as "spherelike" and "disklike," respectively. The best-fitting model of Cromer *et al.*[6] suggested that the disklike molecules were not planar, but that the center of the molecule moved along the axis of rotation in order to maximize their distance from the spherelike molecules. As a result, the atomic distribution around the disklike molecules is saddle shaped. $\delta$-nitrogen is isostructural with $\gamma$-oxygen,[9–12] $\beta$-fluorine,[12] and $\delta$-carbon monoxide,[7] and it is the only phase that oxygen and nitrogen share.

While conventional x-ray diffraction can provide only a determination of the time- and space-averaged structures, molecular dynamics studies of the $\delta$-phase have provided information on both the nature of the molecular disorder (i.e., dynamic versus static) and the correlated motion of the molecules. Westerhoff and Feile[13] reported spherical disorder for the spherelike molecules and found that the most favored alignment for the disklike molecules was at 45° to the unit cell faces, but with low energy barriers to rotation and therefore dynamic disorder. Belak *et al.*[4] also found nearly complete 3-dimensional (3D) disorder for the spherelike molecule and nearly complete 2D disorder for the disklike molecule, but with a possible preference for aligning parallel and perpendicular to the unit cell faces. Finally, the extensive studies of Mulder *et al.*[14] concluded that the spherelike molecules have almost complete 3D rotational disorder but with a weak preference for aligning along the $\langle 111 \rangle$ directions, while there was also a slight preference for the disklike molecules to align parallel and perpendicular to the unit cell faces. The Raman study of Scheerboom and Schouten[15] also concluded that the molecules were "more or less freely rotating," and the overall picture from these studies of the $\delta$ phase is one of nearly spherical disorder of the spherelike molecules and of disklike molecules that show a preference for some alignment, but with no agreement about the nature of the orientation. This model is shown in Fig. 2(a).

On further compression the $\delta$ phase transforms to the $\delta^*$ phase, also known as $\delta_{(\mathrm{loc})}$, at 10.5 GPa at ambient temperature.[15] The $\delta^*$ phase was first discovered by Scheerboom and Schouten[15] from the changing gradient of the spherelike molecule's vibron frequency with pressure. An

[a]Electronic mail: g.stinton@ed.ac.uk.

 

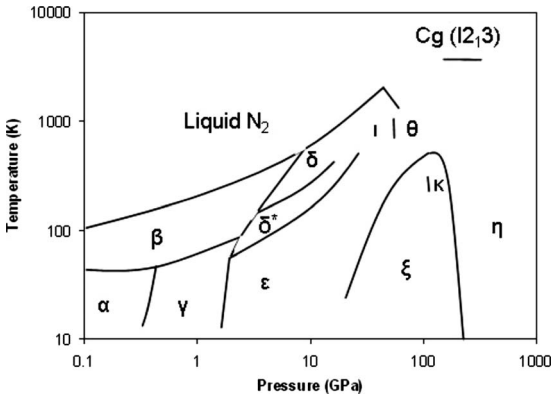


FIG. 1. Phase diagram of nitrogen adapted from Refs. 20 and 26. Note the logarithmic scales.

x-ray powder diffraction study by Hanfland *et al.*[16] observed numerous additional reflections appearing at the transition to the $\delta^*$ phase, indicating that the $\delta^*$ phase has an enlarged tetragonal unit cell with space group $P4_2/ncm$ and cell dimensions of $a_{\delta^*}=\sqrt{2}a_\delta$ and $c_{\delta^*}=a_\delta$, and therefore 16 molecules per unit cell. A good fit to the x-ray diffraction data was obtained by using a combination of ordered and disordered molecules. The basic molecular structure of the $\delta^*$ phase is shown in Fig. 2(b).

Despite the excellent quality of the x-ray data of Hanfland *et al.*,[16] subsequent spectroscopic and theoretical studies have proposed different symmetries for the $\delta^*$ phase. The tetragonal structure proposed by Hanfland *et al.* for the $\delta^*$ phase was predicted by Bini *et al.*[17] to have eight vibronic Raman modes and two infrared (IR) modes, whereas the observed spectrum[17–19] has only two Raman modes (one associated with the spherelike and one with the disklike molecules) and a single IR mode (associated with the disklike molecules). In order to explain their observations, Bini *et al.*[18] favored a 32-molecule cubic structure, although this would still give three Raman modes. Hellwig *et al.*[19] suggested that the $\delta^*$ phase is a tetragonal distortion of the basic eight-molecule $\delta$-structure with the additional modes generated being either degenerate or too weak to detect. Theoretical work by Katzke and Tolédano[20] favored the enlarged 16-molecule unit cell of Hanfland *et al.*, but with C-centered orthorhombic rather than tetragonal symmetry, while the Monte Carlo calculations of Mulder *et al.*[14] favored a 64-molecule structure.

It is surprising that in a system as basic as nitrogen there are still fundamental disagreements over the structures of the lower-pressure phases and the nature of the disorder of the molecules. Of particular surprise is the disagreement between x-ray, spectroscopic and computational studies of the $\delta^*$ phase. To address these issues, we have employed modern single-crystal x-ray diffraction techniques utilizing synchrotron radiation to make detailed structural studies of both the $\delta$ and $\delta^*$ phases, focusing in particular on the nature of the molecular disorder and the structure of the $\delta^*$ phase.

## II. EXPERIMENTAL DETAILS

The nitrogen samples were loaded cryogenically into two Merrill–Bassett-type diamond anvil cells equipped with large-aperture ($4\theta=75°$) Boehler-Almax seats[21] and diamond anvils with 400 $\mu$m culets. A small piece of ruby was included with the sample for pressure measurement via the ruby fluorescence method[22] using the scale of Mao *et al.*[23] To produce a single crystal of the $\delta$ phase, the sample was pressurized to 5.0 GPa and annealed at 70 °C for 11 h before cooling it slowly (12 h) back to room temperature. The final sample pressure was 5.7 GPa, and the single crystal of the $\delta$ phase completely filled the gasket hole. To produce a single crystal of the $\delta^*$ phase, a second sample was first pressurized to 15.0 GPa before annealing at 400 °C for 2 weeks followed by slow cooling back to ambient temperature. The final pressure was 14.5 GPa. This method produced a small number (~8) of high quality crystals of the $\delta^*$ phase, the largest of which was ~60 $\mu$m in diameter.

Two data sets were collected from the $\delta$ crystal. The first was recorded on beamline 9.5HPT at the Synchrotron Radiation Source (SRS), Daresbury Laboratory, utilizing a wavelength of 0.44 Å and a Mar345 image plate detector placed at ~350 mm from the sample. The second data set was obtained on beamline ID27 at the European Synchrotron Radiation Facility (ESRF), Grenoble using a wavelength of 0.37 Å and a MarCCD detector placed at ~160 mm from the sample. The incident x-ray beam diameters [full width at half maximum (FWHM)] were ~25 $\mu$m at the SRS and ~5 $\mu$m at the ESRF. Data were collected out to minimum *d*-spacings of 0.950 and 0.775 Å, respectively. The SRS data were collected in a sequence of contiguous 0.25° oscillations over a total scan range of 70° around the vertical axis. The exposure time of 4 s per frame was chosen to ensure that the strongest reflections did not saturate the detector. For the ESRF data collection, the diffraction data were collected in a sequence of contiguous 0.25° oscillations over a total scan range of 50° around the vertical axis. The exposure time of

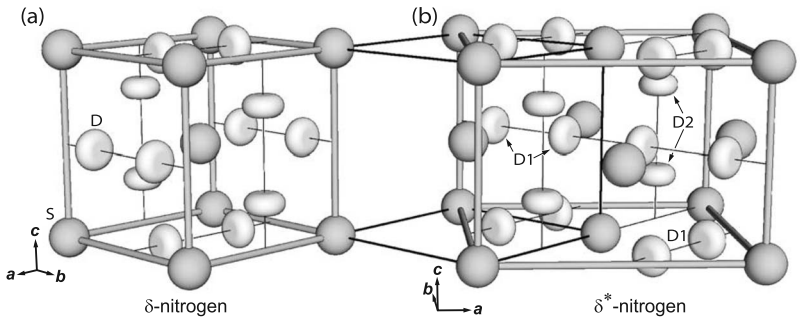


FIG. 2. Schematic view of the basic crystal structures of (a) the $\delta$-phase (Ref. 6) and (b) the $\delta^*$-phase of nitrogen (Ref. 16). Spheres (S) represent 3D disordered, quasispherical molecules and oblate spheres represent two-dimensionally disordered, disklike (D) molecules. The rods mark the unit cells and the medium black lines highlight the relation between the phases.

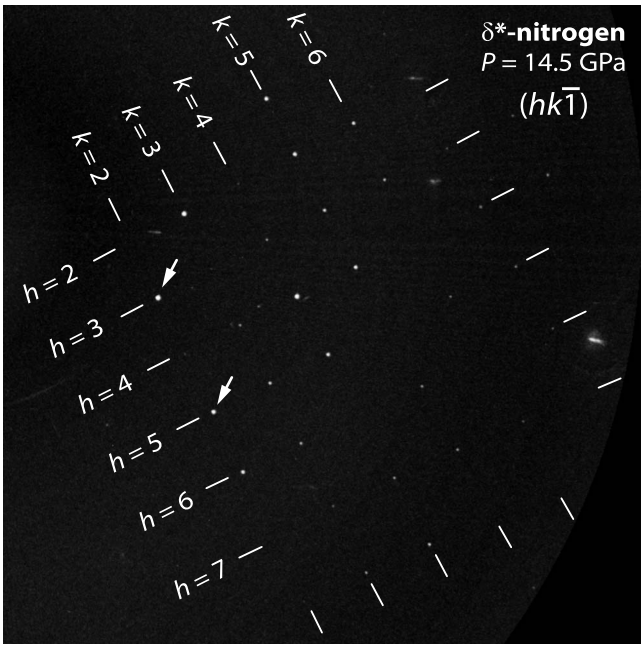


FIG. 3. Single-crystal diffraction image of $\delta^*$-nitrogen at 14.5 GPa. The image shows part of a composite image comprising 24 superimposed diffraction images covering an 8° angular scan range. A nonlinear intensity scale was used to show the weaker reflections more clearly. As discussed in the text, the $(32\bar{1})$ and $(52\bar{1})$ reflections marked by arrows are clearly observable.

10 s per frame was chosen such that the weak, high-angle reflections were measured with good counting statistics. This meant that the strongest Bragg reflections were saturated.

Diffraction data from the $\delta^*$ phase were collected on beamline ID09a at the ESRF using a wavelength of 0.41 Å and a Mar345 image plate detector placed at ~200 mm from the sample. Diffraction data were collected out to a minimum $d$-spacing of 0.775 Å. The incident x-ray beam was ~10 $\mu$m in diameter (FWHM), significantly smaller than the crystal size of ~60 $\mu$m, thereby ensuring that the data were collected from only one of the crystals in the sample. To ensure that the beam was centered on the chosen crystal, a ±30° oscillation diffraction pattern was taken at each position in a $5\times5$ rastering pattern with a step size of 10 $\mu$m. Analysis of these raster scans enabled the location of the different crystals to be determined and ensured that the x-ray beam was centered on only one of these during the final data collection. The diffraction data were collected in a sequence of contiguous 0.333° oscillations over a total scan range of 70° around the vertical axis. To increase the completeness of the data, a second data set was collected with the sample rotated 90° around the x-ray beam and otherwise identical settings. An exposure time of 2 s per frame was chosen to ensure that the strongest reflections were not saturated. An example of the diffraction data is given in Fig. 3.

## III. UNIT CELL AND SPACE GROUP DETERMINATION

The unit cell and orientation matrix of the $\delta$-phase crystal were refined from the positions of 51 reflections from the ESRF data and revealed the structure to be cubic with a lattice parameter of $a=6.112(4)$ Å at 5.7 GPa and 293 K. The intensities of all accessible reflections were integrated using the SAINT+ program[24] and were corrected for decay of the intensity of the x-ray beam, changes in the illuminated sample volume due to the sample rotation, and absorption by the diamond anvils. No correction was made for the absorption of the sample. A total of 611 individual reflections were accessible in the two data sets, and analysis of the systematic absences showed them to be consistent with the centrosymmetric space group $Pm\bar{3}n$ and the noncentrosymmetric $P\bar{4}3m$. Dunstetter and Delapalme[10] favored the space group $Pm\bar{3}n$ over $P\bar{4}3m$ due to the former having an inversion center on the $2a$ position, generating a whole molecule passing through the origin. Cromer *et al.*[6] also favored $Pm\bar{3}n$. Merging of the data sets and averaging of symmetry-equivalent reflections gave 66 independent reflections with an internal intensity agreement $R_{\text{merge}}$ of 5.2%.

The unit cell and orientation matrix of the $\delta^*$-phase were refined from the positions of 78 reflections and revealed it to be tetragonal with lattice parameters of $a=8.063(5)$ Å and $c=5.685(5)$ Å at 14.5 GPa and 293 K; giving a $c/a$ ratio of 1.419(1). The intensities of all accessible reflections were integrated and corrected as for the $\delta$-phase. A total of 1645 individual reflections were accessible and analysis of the systematic absences showed them to be consistent with only one space group, $P4_2/ncm$. The systematic absences are shown in Table I. Of particular note is the clear observation of the (321) and (521) reflections, together with eight of the symmetry equivalents of both reflections, as shown in Fig. 3. These rule out both the *Cccm* structure proposed by Katzke and Tolédano[20] and the cubic unit cell proposed by Hellwig

TABLE I. Systematic reflection absences of $\delta^*$ nitrogen. Only space group $P4_2/ncm$ satisfies the observed absences.

| | Condition | Observed reflections | Unobserved reflections | Complementary condition | Observed reflections | Unobserved reflections | Total | Condition is … |
|---|---|---|---|---|---|---|---|---|
| $hkl$ | $h+k+l$=even | 47 | 37 | $h+k+l$=odd | 27 | 55 | 166 | Violated |
| $hk0$ | $h+k$=even | 19 | 10 | $h+k$=odd | 0 | 23 | 52 | Met |
| $h0l$ | $l$=even | 9 | 7 | $l$=odd | 0 | 11 | 27 | Met |
| $h0l$ | $h$=even | 6 | 8 | $h$=odd | 3 | 10 | 27 | Violated |
| $h0l$ | $h+l$=even | 6 | 7 | $h+l$=odd | 3 | 11 | 27 | Violated |
| $hhl$ | $l$=even | 7 | 5 | $l$=odd | 4 | 4 | 20 | Violated |
| $h00$ | $h$=even | 4 | 1 | $h$=odd | 0 | 5 | 10 | Met |
| $hh0$ | $h$=even | 3 | 0 | $h$=odd | 4 | 0 | 7 | Violated |
| $00l$ | $l$=even | 0 | 0 | $l$=odd | 0 | 0 | 0 | Unknown |

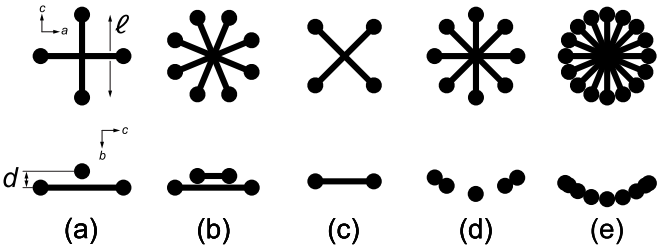


FIG. 4. Arrangement of equivalent Wyckoff sites for the (a) 24*k*, (b) 48*l*, (c) 24*j*, (d) 24*j*+24*k*, and (e) 24*j*+24*k*+48*l* models of the disklike molecule of the $\delta$-phase. The top row shows the view looking perpendicular to the plane of the molecules, i.e., down the *b*-axis for the molecule labeled D in Fig. 2(a), while the bottom row shows the view parallel to the plane of the molecules, i.e., down the *a*-axis.

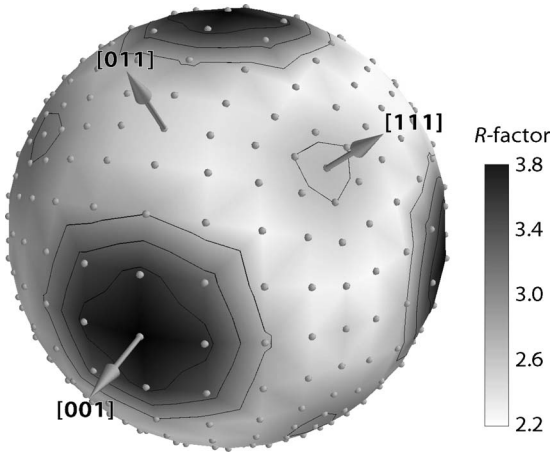


FIG. 5. Representation of the quality of fit obtained for different orientations used in the multisite modeling of the spherelike molecules in the $\delta$-phase of nitrogen. Each point on the sphere represents a refinement with the nitrogen molecule aligned along that direction with the resulting *R*-factor represented by a grey scale running from white (best fit) to black (worst fit). Contour lines are shown at *R*-factors of 2.6, 3.0, and 3.4.

*et al.*[19] Our data are, however, completely consistent with the unit cell and space group proposed by Hanfland *et al.*[16] Following Hanfland *et al.*, origin choice 2 was selected. Merging of symmetry-equivalent reflections from both data sets gave 166 independent reflections and an $R_{\text{merge}}$ of 6.6%.

### A. Structure of the $\delta$-phase

The structure refinements of both the $\delta$ and $\delta^*$ phases were performed using the TOPAS ACADEMIC software package.[25] The orientational disorder of the molecules in the $\delta$ phase was modeled and analyzed in the style of the work by Cromer *et al.*[6] For the spherelike molecules two different models were used. These are (I) freely rotating molecules using the spherical $N_2$ form factor of Cromer *et al.* and (II) a multisite disordered model with $\frac{1}{4}$ occupied sites located on the 16*i* $(x,x,x)$ Wyckoff positions. In addition, five different models were used for the disklike molecules, as shown in Fig. 4. The first two models are those used by Cromer *et al.* and are (a) $\frac{1}{2}$-occupied N sites located on the 24*k* position and (b) $\frac{1}{4}$-occupied sites located on the 48*l* positions. The third model (c) is closely related to (a) but uses the 24*j* positions and involves a rotation of the $N_2$ molecules by 45°. Model (d) combines models (a) and (c), and model (e) combines (a), (b), and (c).

In the multisite models for the disklike molecules, correlations between parameters prevented the free refinement of all atomic coordinates. In each of the five models for the disklike molecules, only two parameters were refined—the distance between the atoms in the same molecule (labeled "*l*" in Fig. 4(a)) and the distortion of the disk away from its nearest neighbors (labeled "*d*" in Fig. 4(a)). All atomic positions where determined from these two parameters. In all cases, a single isotropic atomic displacement parameter was refined. The results are summarized in Table II. The best fit is obtained with model I(d), i.e., the combination of a fully spherical molecule and a disklike molecule taking four different orientations. It should be noted that the fits with models I(b) and I(e) are only marginally inferior.

Unlike Cromer *et al.*, or the study of isostructural $\gamma$-$O_2$ by Cox *et al.*,[9] the best fit to the $\delta$-phase data is achieved using a freely rotating molecule for the spherelike molecule—model I—rather than aligning molecules along the ⟨111⟩ directions. Following the work of Dunstetter and Delapalme[10] we determined whether a still better fit might be obtained by modeling the spherelike molecules with partially-occupied sites in orientations other than the ⟨111⟩ directions. The results are summarized in Fig. 5. During all refinements, model (d) was used for the disklike molecules with disorder over the 24*j* and 24*k* sites. The poorest fit with an *R*-factor of 3.792% was obtained with the spherelike molecules aligned along ⟨001⟩. A second unfavorable direction is ⟨111⟩. These are the directions of the nearest and second-

TABLE II. Summary of the different models used for describing the structure of the $\delta$ phase of nitrogen.

| Model | Spherelike site | Occupancy | Disklike site | Occupancy | Parameters | *R*-factor |
|---|---|---|---|---|---|---|
| I(a) | 2*a* (0,0,0) | Spherical $N_2$ | 24*k* | $\frac{1}{2}$ N atom | 5 | 4.334 |
| I(b) | 2*a* (0,0,0) | Spherical $N_2$ | 48*l* | $\frac{1}{4}$ N atom | 5 | 2.199 |
| I(c) | 2*a* (0,0,0) | Spherical $N_2$ | 24*j* | $\frac{1}{2}$ N atom | 4 | 6.882 |
| I(d) | 2*a* (0,0,0) | Spherical $N_2$ | 24*k*+24*j* | $\frac{1}{4}$ N atom | 5 | 2.166 |
| I(e) | 2*a* (0,0,0) | Spherical $N_2$ | 48*l*+24*k*+24*j* | $\frac{1}{8}$ N atom | 5 | 2.180 |
| II(a) | 16*i* $(x,x,x)$ | $\frac{1}{4}$ N atom | 24*k* | $\frac{1}{2}$ N atom | 6 | 5.067 |
| II(b) | 16*i* $(x,x,x)$ | $\frac{1}{4}$ N atom | 48*l* | $\frac{1}{4}$ N atom | 6 | 2.647 |
| II(c) | 16*i*$(x,x,x)$ | $\frac{1}{4}$ N atom | 24*j* | $\frac{1}{2}$ N atom | 5 | 7.195 |
| II(d) | 16*i* $(x,x,x)$ | $\frac{1}{4}$ N atom | 24*k*+24*j* | $\frac{1}{4}$ N atom | 6 | 2.663 |
| II(e) | 16*i* $(x,x,x)$ | $\frac{1}{4}$ N atom | 48*l*+24*k*+24*j* | $\frac{1}{8}$ N atom | 6 | 2.825 |

nearest neighbors, respectively. Apart from these two directions and those immediately adjacent to them, the quality of fit is similar. The best fit to the data is obtained with molecules pointing in the ⟨304⟩ and ⟨314⟩ directions with an *R*-factor of 2.232%. We note, however, that this fit is still poorer than that obtained with a freely rotating molecule.

There was very little difference to the quality of fit if the disklike molecule models (b) and (e) are combined with ⟨314⟩ orientations at the spherelike site, giving $R=2.238\%$ and 2.233%, respectively. For the ⟨304⟩ model, $R=2.292\%$ and 2.287% when combined with models (b) and (e), respectively.

Additional refinements were carried out using a freely rotating molecule, combined with molecules aligned along ⟨001⟩. The total occupancy was fixed to two N atoms per sphere but the relative occupancies of "rotating" and "disordered" molecule were subject to refinement. The *R*-factor improved significantly to 2.065% with the occupancy of the disordered molecule becoming negative (−0.0919). This result supports the idea of near-free rotational disorder, but with the molecules showing a preference for avoiding the ⟨001⟩ direction. A similar refinement that combined a freely rotating molecule with another aligned along the ⟨111⟩ directions did not improve the fit.

Our results therefore suggest that the best model for the spherelike molecules of the $\delta$ phase is a spherically rotating molecule with a certain preference for avoiding pointing along the ⟨001⟩ directions. This result is in agreement with the study of isostructural $\gamma$-oxygen by Dunstetter and Delapalme[10] who also found the ⟨001⟩ directions unfavorable.

Refinements of the $\delta$ phase using the five different models for the disklike molecules showed little difference in the quality of fit between models (b), (d), and (e)—the three that give the largest spread of atomic positions around the disk. This agrees with the previous studies of Cromer *et al.*[6] and Cox *et al.*[9] who both favored model (b) over model (a). We conclude, therefore, that the disklike molecules are able to rotate, as discussed by Westerhoff and Feile.[13]

### B. Structure of the $\delta^*$-phase

Due to the similarity of the diffraction patterns of the $\delta$ and $\delta^*$ phases, the two structures are expected to be closely related. The positions of the molecular centers are the same for the $\delta$ phase and the ordered $\varepsilon$ phase of Mills *et al.*[7] when the latter is transformed into a rhombohedral setting, suggesting that the molecules will be in the same positions in the intermediate $\delta^*$ phase. Therefore, our starting point for refinement of the $\delta^*$ structure was the conversion of the best-fitting model I(d) for the $\delta$ phase described above into $P4_2/ncm$ symmetry and the larger unit cell of the $\delta^*$ phase. This conversion results in the $\delta^*$ phase having three symmetry-independent molecules, one derived from the spherelike molecules with four symmetry equivalents (henceforth labeled ex-sphere) and two derived from the disklike molecules in a ratio of 8:4 (labeled ex-disk 1 and ex-disk 2, respectively).

Directly transforming the best-fitting I(d) structure of the $\delta$ phase (Table II) into the $\delta^*$ unit cell gave a large *R*-factor of 14.79%. While this model fitted the intense, low-angle reflections well, it predicted zero intensity for the clearly visible (321) and (521) reflections. The disklike molecules in the $\delta^*$ structure are expected to be more ordered than in the $\delta$ phase;[14] therefore models were needed which allowed greater localization. Transforming the disksite model (e) from the $\delta$ phase into $P4_2/ncm$ gave eight symmetry-independent sites for ex-disk 1 molecules and five sites for ex-disk 2 molecules (with two sites on 8*i* positions rather than general positions). The sites are shown in Figs. 6(b) and 6(c). Model (e) was chosen over model (d) due to the greater number of sites allowing greater flexibility to model the $\delta^*$ structure.

The positions of the atoms were controlled by two refinable parameters per ex-disk molecule, as in the $\delta$ phase. The first was the distance between atoms related by the inversion center at the center of the disk, and the second modeled the distortion of the disk away from its nearest neighbors. The occupancies of various sites were allowed to refine but the total occupancy of each ex-disk was fixed at 2. This gave $R=8.005\%$, an improved but still unconvincing fit. Therefore, a similar type of modeling was introduced for the ex-sphere molecules. Refinements were carried out using all of the different orientations shown in Fig. 5 converted into $P4_2/ncm$ symmetry. This generated either 3, 4, or 6 symmetry-independent sites for the $(0,0,x)$, $(x,x,x)$, and $(x,y,z)$ alignments of molecules, respectively. The occupancies of these sites were refined with the total occupancy again fixed at 2.

In the best-fitting model, the ex-sphere molecules are aligned along what were the 24 symmetry equivalent ⟨112⟩ directions in the $\delta$ phase. Converting this into space group $P4_2/ncm$ generates six symmetry-inequivalent directions. These are the $\langle 01\sqrt{2}\rangle$, $\langle 0\bar{1}\sqrt{2}\rangle$, $\langle 13\sqrt{2}\rangle$, $\langle \bar{3}\bar{1}\sqrt{2}\rangle$, $\langle \bar{1}3\sqrt{2}\rangle$, and $\langle \bar{3}1\sqrt{2}\rangle$ directions, each with four symmetry equivalents. This model results in an *R*-factor of 2.126% with the occupancy of four sites (11, 15, 17, and 22—see Fig. 6) refining to zero. These sites were then removed from the model. Three other sites (5, 16, and 23) also had very low occupancy (<0.04), and removing these resulted in a further slight decrease in the *R*-factor to 2.115% and a decrease in the number of refined parameters from 20 to 17. The final structural model for the $\delta^*$ phase is shown in Fig. 7 with details in Fig. 6 and atomic coordinates listed in Table III.

The unit cell, space group symmetry, and molecular centers determined for the $\delta^*$ phase are in complete agreement with the previous study of Hanfland *et al.*[16] The ex-sphere molecules weakly favor aligning along the $\langle \bar{3}\bar{1}\sqrt{2}\rangle$ directions and preferentially avoid the $\langle 01\sqrt{2}\rangle$ direction, but still with a large amount of disorder. This partial ordering can be seen as an intermediate state of disklike disorder between the almost-spherical distribution of the same molecules in the $\delta$-phase and the alignment of the molecules along the ⟨111⟩ directions in the ordered $\varepsilon$-phase.[20]

The ex-disk 1 molecules librate around a position at ±45° to the *ab* face of the cubic $\delta$-phase unit cell (see Figs. 6 and 7), which can be compared to the angles of ±35° and

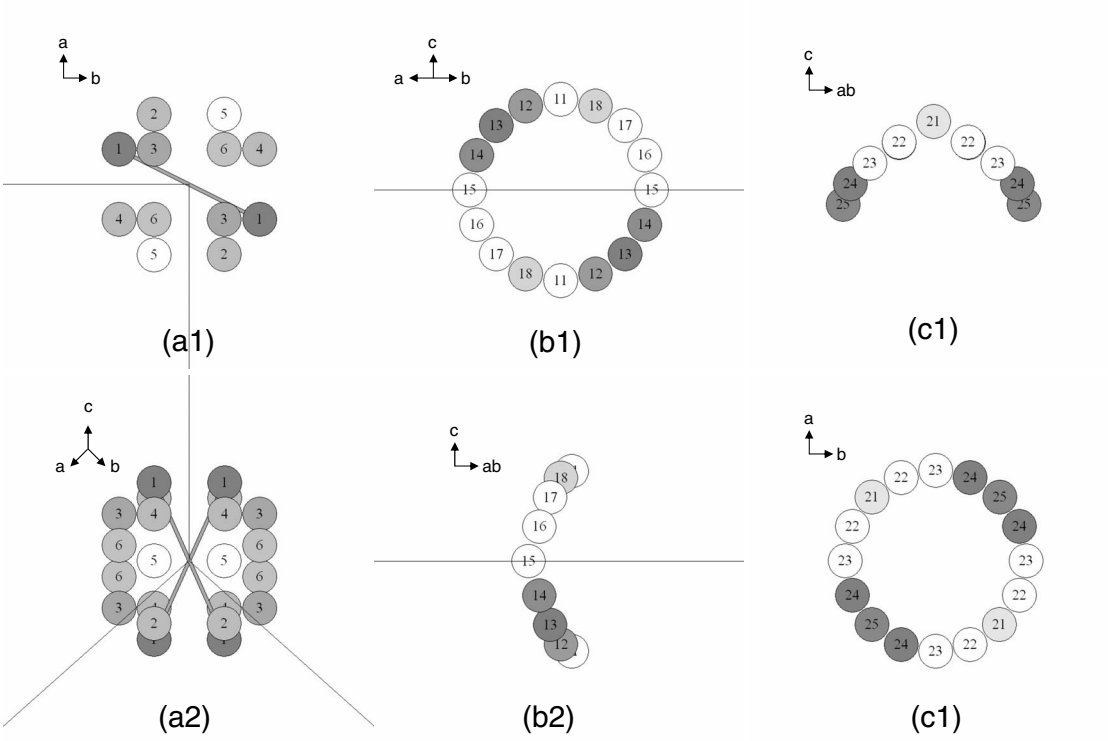


FIG. 6. Details of the $\delta^*$-nitrogen molecules showing occupied sites in gray, with darker shades for more heavily occupied sites, and unoccupied sites in white. Figures (a1) and (a2) show the ex-sphere at (0,0,0) viewed along the [001] and [112] directions, respectively. Figures (b1) and (b2) show ex-disk 1 at $(\frac{5}{8},\frac{1}{8},0)$ viewed along the [110] and $[1\bar{1}0]$ directions, respectively. Figures (c1) and (c2) show ex-disk 2 at $(\frac{3}{4},\frac{3}{4},\frac{3}{4})$ viewed along the $[1\bar{1}0]$ and [001] directions, respectively.

$\pm 50°$ calculated by Mulder *et al.*[14] About 11% of the occupancy is at positions at 90° to this, suggesting a very hindered rotation around the disk. The ex-disc 1 molecules can be thought of as forming chains with their nearest neighbors in either the [110] or $[1\bar{1}0]$ direction along the axis of libration. The *orientations* of the molecules are paired along the chains (as illustrated in Fig. 7, most easily seen along the $[1\bar{1}0]$ direction in the $c=\frac{1}{2}$ plane). There are four next-nearest neighbors. Two are in the ⟨001⟩ directions (all with identical orientations) and two in the *c*-plane, 90° to the axis of libration (with alternating orientations). The partial alignment of the molecules can be seen as a step toward the fully-aligned chains in the $\varepsilon$-phase.

The ex-disk 2 molecules librate around a position aligned with face diagonals of the $\delta^*$ unit cell (and hence parallel with the edges of the $\delta$ cell) with alternate molecules along the chain perpendicular to one another, as required by

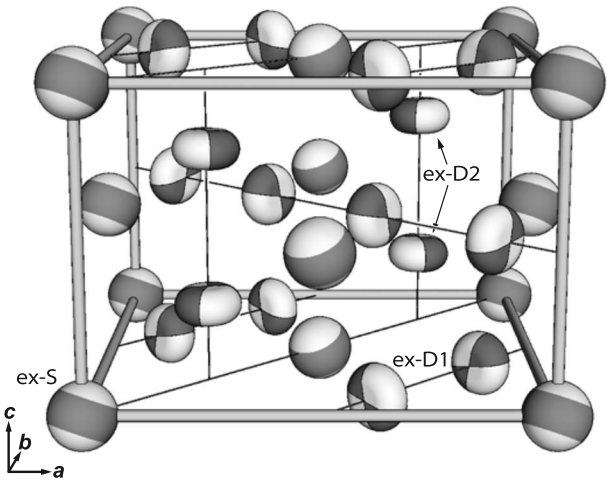


FIG. 7. Schematic view of the refined crystal structure of $\delta^*$-nitrogen. Spheres represent the more 3D disordered molecules (ex-spheres or ex-S) and the oblate spheres represent the ex-disk molecules (ex-D1 and ex-D2). The dark areas indicate the preferred orientations of the molecules.

TABLE III. Final atomic positions for the $\delta^*$ phase at 14.5 GPa.

| Atom number | Coordinates | | | Occupancy |
|---|---|---|---|---|
| | *x* | *y* | *z* | |
| Ex-sphere | | | | |
| 1 | 0.0536(6) | 0.0179(6) | −0.0358(5) | 0.15(3) |
| 2 | 0 | −0.0358(3) | 0.071(1) | 0.08(2) |
| 3 | 0.0537(5) | −0.0179(6) | −0.0358(5) | 0.11(2) |
| 4 | 0.0179(5) | 0.0537(6) | 0.0358(5) | 0.08(1) |
| 6 | −0.0179(5) | 0.0537(6) | 0.0358(5) | 0.07(2) |
| Ex-disk 1 | | | | |
| 12 | 0.1484(4) | 0.6128(4) | 0.0860(5) | 0.26(2) |
| 13 | 0.1579(2) | 0.5920(2) | 0.0658(4) | 0.33(3) |
| 14 | 0.6624(4) | 0.4236(4) | 0.4643(6) | 0.29(2) |
| 18 | 0.8516(4) | 0.3872(4) | 0.0860(5) | 0.114(7) |
| Ex-disk 2 | | | | |
| 21 | 0.2038(7) | 0.2962(7) | 0.207(1) | 0.063(6) |
| 24 | 0.7250(4) | 0.8103(4) | 0.2288(7) | 0.32(1) |
| 25 | 0.2039(7) | 0.2961(7) | 0.792(2) | 0.30(3) |

the $4_2$ screw axis of the space group. The molecules in neighboring chains are also perpendicular to one another. Due to the experimentally determined unit cell being at 45° to that modeled by Mulder *et al.*, this corresponds to their angle of 0° or 90° to the cell edge with the same pattern of alternating orientations.

## IV. CONCLUSION

Using high-pressure single crystal techniques and synchrotron radiation, we have investigated the structures of the $\delta$ and $\delta^*$ phases of nitrogen. In contrast to the previous x-ray study of the $\delta$ phase, our results suggest that the best model for the spherelike molecules of the $\delta$ phase is a spherically rotating molecule, which has a certain preference for avoiding pointing along the $\langle 001 \rangle$ directions. This result is in agreement with the study of isostructural $\gamma$-oxygen by Dunstetter and Delapalme,[10] who also found the $\langle 001 \rangle$ directions unfavorable, and the molecular dynamic studies of the $\delta$ phase all of which favored spherical disorder of these molecules. We find the best model for the "disklike" molecules of the $\delta$ phase to be that in which the molecules are disordered over a large number of sites, in agreement with the previous studies of $\delta$-nitrogen[6] and $\gamma$-oxygen,[9] and suggestive of molecular rotation.[13]

The structure of the $\delta^*$ phase has been unambiguously identified as being tetragonal with space group $P4_2/ncm$, in complete agreement with Hanfland *et al.*[16] Other structures and symmetries proposed in the literature can be rejected.[17–20] The best model for the spherelike molecules of the $\delta^*$ phase is one in which they weakly favor aligning along the $\langle 3\bar{1}\sqrt{2} \rangle$ directions and preferentially avoid the $\langle 01\sqrt{2} \rangle$ direction, but still with a large amount of disorder. The two symmetry-independent sets of disklike molecules of the $\delta^*$ phase are partially aligned, although still undergoing substantial librations, and form chains in which the molecular orientations are either paired or are perpendicular to each other. The molecular orientation is similar to those calculated by Mulder *et al.*[14]

The confirmation of the symmetry and space group of the $\delta^*$ phase still leaves the question as to why far fewer Raman ($R$) and IR modes are observed ($2R$ and 1 IR) compared to those calculated from this structure ($8R$ and 2 IR).[17,18] We note that no structure yet proposed for the $\delta^*$ phase gives the correct number of modes: even the high-symmetry cubic structures proposed by Bini *et al.*[18] have an additional Raman mode. Further studies or understanding are required.

## ACKNOWLEDGMENTS

We thank A. Lennie of Daresbury Laboratory and M. Mezouar, W. Crichton, M. Hanfland, and M. Merlini of the ESRF for their help with the experiments. This work was supported by research grants from U.K. Engineering and Physical Sciences Research Council and facilities were made available by the SRS and the ESRF. The x-ray diffraction experiments at the ESRF were performed as part of Long Term Project HS3090 on single crystal diffraction at extreme conditions.

[1] S. Krukowski and P. Straak, J. Chem. Phys. **124**, 134501 (2006).
[2] E. Gregoryanz, A. F. Goncharov, R. J. Hemley, and H. K. Mao, Phys. Rev. B **64**, 052103 (2002).
[3] M. I. Eremets, A. G. Gavriliuk, I. A. Trojan, D. A. Dzivenko, and R. Boehler, Nature Materials **3**, 558 (2004).
[4] J. Belak, R. Lesar, and R. D. Etters, J. Chem. Phys. **92**, 5430 (1990).
[5] W. Press and A. Hüller, J. Chem. Phys. **68**, 4465 (1978).
[6] D. T. Cromer, R. L. Mills, D. Schiferl, and L. A. Schwalbe, Acta Crystallogr., Sect. B: Struct. Crystallogr. Cryst. Chem. **37**, 8 (1981).
[7] R. L. Mills, B. Olinger, and D. T. Cromer, J. Chem. Phys. **84**, 2837 (1986).
[8] H. Olijnyk, J. Chem. Phys. **93**, 8968 (1990).
[9] D. E. Cox, E. J. Samuelsen, and K. H. Beckurts, Phys. Rev. B **7**, 3102 (1973).
[10] F. Dunstetter and A. Delapalme, Physica B **156**, 112 (1989).
[11] F. Dunstetter, O. H. Duparc, V. P. Plakhty, J. Schweizer, and A. Delapalme, Fiz. Nizk. Temp. **22**, 140 (1996).
[12] T. H. Jordan, W. E. Streib, H. W. Smith, and W. N. Lipscomb, Acta Crystallogr. **17**, 777 (1964).
[13] T. Westerhoff and R. Feile, Z. Phys. B: Condens. Matter **100**, 417 (1996).
[14] A. Mulder, J. P. J. Michels, and J. A. Schouten, Phys. Rev. B **57**, 7571 (1998).
[15] M. I. M. Scheerboom and J. A. Schouten, Phys. Rev. Lett. **71**, 2252 (1993).
[16] M. Hanfland, M. Lorenzen, C. Wassilew-Reul, and F. Zontone, Rev. High Pressure Sci. Technol. **7**, 787 (1998).
[17] R. Bini, L. Ulivi, J. Kreutz, and H. J. Jodl, J. Chem. Phys. **112**, 8522 (2000).
[18] R. Bini, M. Jordan, L. Ulivi, and H. J. Jodl, J. Chem. Phys. **108**, 6849 (1998).
[19] H. Hellwig, W. B. Daniels, R. J. Hemley, H. K. Mao, E. Gregoryanz, and Z. H. Yu, J. Chem. Phys. **115**, 10876 (2001).
[20] H. Katzke and P. Tolédano, Phys. Rev. B **78**, 064103 (2008).
[21] R. Boehler and K. De Hantsetters, High Press. Res. **24**, 391 (2004).
[22] G. J. Piermarini, S. Block, J. D. Barnett, and R. A. Forman, J. Appl. Phys. **46**, 2774 (1975).
[23] H. K. Mao, J. Xu, and P. M. Bell, J. Geophys. Res., [Solid Earth] **91**, 4673 (1986).
[24] SAINT+ Integration Software, Bruker AXS, 1997.
[25] TOPAS ACADEMIC software v4.1, A. A. Coelho, Brisbane, Australia, 2007.
[26] E. Gregoryanz, A. F. Goncharov, C. Sanloup, M. Somayazulu, H. K. Mao, and R. J. Hemley, J. Chem. Phys. **126**, 184505 (2007).